Section A-Research paper

Imaging Modalities in Sino-Nasal Infections With Orbital Affection

Sana Ehab Abdel-Majeed Ibrahim, Amal Mohamed Hasan, Ahmed Abdel-Hameed Mohamed, Ahmed Awad Bessar

Department of Radiodiagnosis, Faculty of Medicine, Zagazig University, Egypt

Email: sana.ehab.rd@gmail.com, s.ihab021@medicine.zu.edu.eg

Abstract

Background: In the past decade, imaging of the paranasal sinuses has progressed from the realm of conventional radiographs (plain films) almost exclusively into the realms of computed tomography (CT) and magnetic resonance (MR) imaging. Technological advances in these two modalities have provided more precise diff erential diagnoses and greater detail about the anatomic extent of disease. It might seem that, with modern imaging techniques, either CT or MR could provide sufficient information for diagnosis and surgical planning in the sinuses. However, CT and MR provide complementary information; each has advantages and potential drawbacks. There are several important considerations when deciding whether to order CT or MR (or both) to evaluate abnormalities of the paranasal sinuses. The remainder of this article focuses on 10 concepts that can be helpful in tailoring an imaging approach to sinus disease.

Keywords: paranasal sinuses, Imaging

Introduction

In the past decade, imaging of the paranasal sinuses has progressed from the realm of conventional radiographs (plain films) almost exclusively into the realms of computed tomography (CT) and magnetic resonance (MR) imaging. Technological advances in these two modalities have provided more precise diff erential diagnoses and greater detail about the anatomic extent of disease ***(1).***

It might seem that, with modern imaging techniques, either CT or MR could provide sufficient information for diagnosis and surgical planning in the sinuses. However, CT and MR provide complementary information; each has advantages and potential drawbacks ***(2).***

Clinicians who understand the relative strengths and weaknesses of CT and MR are able to pursue a more directed approach to imaging. Understanding the most common diagnostic errors associated with each modality is critical to such decision making. There are several important considerations when deciding whether to order CT or MR (or both) to evaluate abnormalities of the paranasal sinuses. The remainder of this article focuses on 10 concepts that can be helpful in tailoring an imaging approach to sinus disease ***(3).***

CT excels at evaluating fine bone detail:

Because cortical bone and air have no signal on MR sequences, an analysis of the normal sinus cavity anatomy is difficult with MR. CT, however, excels at assessing cortical bone. Subtle increases in mucosal thickness can be appreciated on CT because the surrounding air and bone are of such different radiodensities. This concept is particularly evident in the evaluation of the expanded sinus. A thin rim of remodeled bone may be present and yet difficult to assess on MR ***(4).***

MR can provide useful information in the setting of mucocele, but CT provides the best assessment of the bony remodeling and dehiscence. MR imaging of mucoceles is complicated by the variable signal intensity of the mucocele contents. Depending on the degree of desiccation, the T1 and T2 signals may be hyperintense or hypointense ***(5).***

Contrast-enhanced MR may be useful to identify superinfection (mucopyocele). Thickened, enhancing mucosa, with or without enhancement of surrounding soft tissues, is suggestive of this complication. Even in the absence of enhancement, however, increased T1 signal may be used to suggest mucopyocele ***(1).***

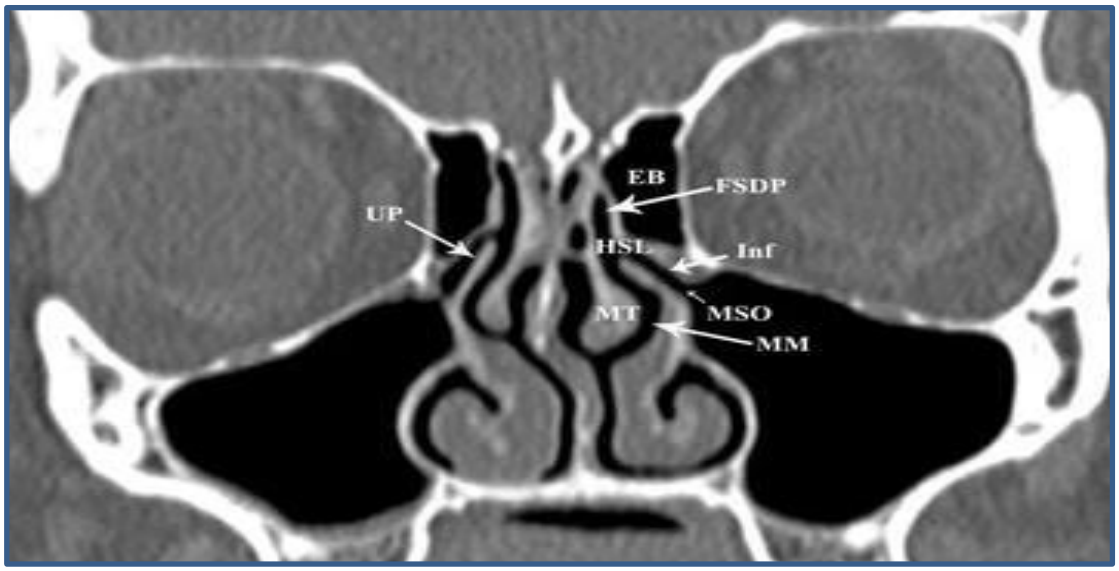

Figure (1): Coronal CT scan demonstrates the structures that comprise to form the ostiomeatal unit (OMU). MM Middle meatus, MSO Maxillary sinus ostium, Inf Infundibulum, HSL Hiatus semilunaris, FSDP Frontal sinus drainage pathway, EB Ethmoid bulla, MT Middle turbinate, UP Uncinate process ***(6).***

MR excels at evaluating soft tissues:

CT is capable of measuring only one property of human tissue: the absorption of X-rays. Although CT assessment can be refined with the use of radiodense contrast agents, the basic physical property remains the same. MR, however, uses varied pulse sequences to interrogate diff erent aspects of the tissues. This is particularly useful for the evaluation of soft tissues, as the diff erent pulse sequences provide a more detailed evaluation of diff erent tissues ***(7).***

With CT, it is often difficult to distinguish proteinaceous fluid from solid material, but MR sequences allow the assessment of various fluid compositions. MR often allows scar tissue to be more readily distinguished from surgical material and recurrent tumors ***(8).***

In the setting of skull base defects, CT may have difficulty distinguishing between scar tissue, mucocele, meningocele, and encephalocele. Although CT cisternography can help to narrow this diff erential, MR can do so without an interventional procedure. Coronal T2-weighted images are particularly useful for this evaluation ***(7).***

Conventional radiographs are of limited diagnostic use:

CT has replaced conventional radiographs as the imaging modality of choice for the assessment of sinusitis. Conventional films have poor sensitivity for mucosal disease in the maxillary sinuses, and worse sensitivity in the other paranasal sinuses. In many authors' opinion, if the sinuses are worth imaging, it is worth using CT ***(1).***

Even as a screening tool for acute rhinosinusitis, conventional radiographs are falling out of favor. Because CT has become ubiquitous, and modern techniques allow for lower patient radiation dose and more comfortable patient positioning, CT is now a more reasonable choice for screening. At some institutions, there is little or no cost diff erence between a screening CT (which consists of thick axial images only) and a series of conventional sinus radiographs ***(2).***

I. Imaging of the orbit

CT:

CT measures the absorption values of different tissues after their exposure to highly collimated x-ray beam. CT is superior for imaging calcification, as in cases of ON head drusen (bone windows), and frequently calcified tumors, such as retinoblastoma and ONS meningioma (ONSM).5 There are notable disadvantages of CT that obscure visualization around the optic canal ***(9).***

In orbital imaging, an axis parallel to the infraorbitomeatal line (ensuring a view parallel to the orbital axis) is essential in axial view to visualize the ON, the MR and LR muscles, and lens in a single slice. High-resolution CT with 1-mm or less slices in the axial, sagittal and coronal plane with corresponding bone windows is the way to image the optic canal ***(10).***

MRI:

MRI is the test of choice for the vast majority of neuro-ophthalmologic disorders with orbital involvement. The ability to image fine details and subtle lesions in the orbit is limited by the large amount of orbital fat. The retro-orbital fat has a strong signal on T1-weighted images (T1WI) that further obscures visualization of gadolinium ***(11).***

Thus, two fat-suppression (FS) techniques have become routine in daily practice: the short tau inversion recovery (STIR) and the selective partial inversion recovery (SPIR). Both of these techniques can be applied to T1WI or T2-weighted images (T2WI). SPIR is superior to STIR in that it selectively inverts the signal from fat without disturbing the signal from water ***(8).***

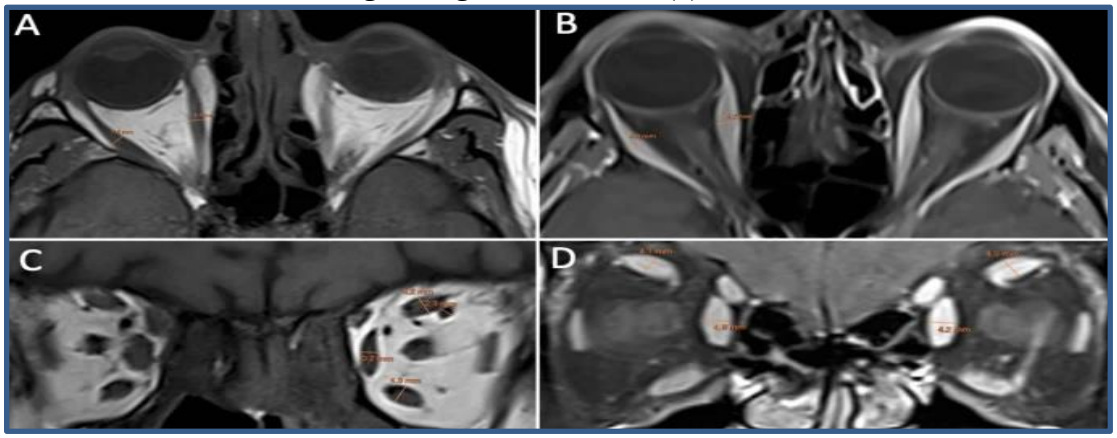

Figure (2): Axial T1-weighted MRI (A) and fat-suppressed contrast enhanced T1-weighted MRI (B) showing the measurements of the right medial and lateral rectus muscles perpendicular to the muscle belly. Coronal T1-weighted MRI (C) showing the measurements of the superior muscle group, medial rectus, inferior rectus and superior ophthalmic vein. Fat-suppressed contrast enhanced T1-weighted MRI (D) showing the measurements of the medial rectus and superior muscle group ***(12).***

Both of these techniques are able to detect pathology embedded in dense orbital fat. The disadvantage of FS technique is an increase in suppression artifact, particularly around metallic implants and dental fillings. This results in failure to suppress normal fat, causing increased signal intensity and mimicking pathology ***(11).***

This artifact is particularly troublesome around aerated sinuses, such as the sphenoid sinus, or close to the optic foramen. On the other hand, conventional MRI has difficulty differentiating between the three main layers of the healthy globe: sclera, uvea, and retina. MRI is able to differentiate the cornea, anterior and posterior chambers, iris, and lens with its capsule, vitreous, and components of the uveal tract. After contrast administration, the vascular structures, in particular the uvea and macula, are depicted by their strong contrast enhancement ***(1).***

Optical coherence tomography (OCT):

Optical coherence tomography (OCT) uses near-infrared light to measure the thickness of different ocular structures, such as the retinal nerve fiber layer (RNFL) and macula. OCT has been shown to capture retinal ganglion cell axon loss in anterior visual pathway disorders, such as glaucoma, ischemic optic neuropathy, optic neuritis, and chiasmal lesions ***(13).***

Ultrasonography:

Traditional, real time A- and B-mode ultrasonography often is helpful in distinguishing thyroid from other myopathies. It differentiates between pseudo- and true optic disc swelling by detecting buried drusen of the ON head ***(14)***

Color Doppler imaging (CDI) is a duplex scan that is capable of simultaneous B-mode imaging and Doppler spectral analysis, showing fine arterial and venous structures. In the orbit, CDI has been reported to be useful in the diagnosis and monitoring of vascular lesions, such as carotid-cavernous fistula (CCF), orbital varices, and the vascular supply of mass lesions ***(10).***

CDI is non-invasively capable of following the spontaneous course, effects of embolization, or occlusion of the fistula. CDI showed that cavernous hemangiomas of the orbit have little to almost no flow. Contrary to this, lymphomas and metastatic lesions of the orbit have large arterial and venous supply ***(14)***

Fluorescein angiography (FA):

Fluorescein angiography (FA) of the globe is able to differentiate between true versus pseudoswelling of the ON head. In a pathologically swollen disc, FA shows fluorescein leak in the late phase of the angiogram. In pseudoswelling, there is staining but no leakage of the dye from the optic disc. In giant cell arteritis (GCA), FA is able to identify retinal and choroidal ischemia, which may represent the first ocular manifestation of the disease ***(10).***

CT and/or MRI are used in characterization and determination of the extent of PNS disease and its complications. CT of the PNS is typically performed without contrast agents. CT provides much better detailed bony anatomy and is valuable for determining anatomic landmarks and variants ***(15).***

CT is helpful to identify erosive processes and acquired developmental deficiencies of the bone. In addition, CT is excellent for determining whether there is intraorbital extension of PNS disease into the anterior two thirds of the orbit. When disease approaches the orbital apex, an MRI scan is indicated to assess spread to the cavernous sinus and intracranial compartment ***(16).***

MRI offers superior and diverse soft tissue contrast resolution and is useful in delineating the extent of disease in more detail. Therefore, MRI is extremely helpful to evaluate PNS complications. First, MRI can discern secretions and mucosa from mass lesions; the signal intensity of secretions can vary and mainly depends on the water-to-protein ratio and viscosity. Second, MRI is useful for determining invasion of the skull base and osseous structures ***(17).***

Finally, MRI is the study of choice for detecting intracranial extension of PNS disease. An MRI protocol of the orbit should include studies with and without contrast and at least coronal fat-saturated T2-weighted (W), axial T1W, and axial and coronal fat-saturated T1W imaging. The MRI protocol should also include diffusion-weighted imaging (DWI) and MR venography in addition to the routine scanning protocols ***(18).***

DWI is an advanced MRI technique that provides image contrast based on differences in diffusion/mobility of water molecules. Diffusion mainly represents the random Brownian motion of water molecules. The apparent diffusion coefficient (ADC) value is an absolute quantitative measurement of translational water mobility, which can be compared in serial examinations ***(17).***

Based upon the different mobility of water molecules in their local environment, DWI generates image contrast; certain pathologic processes restrict water mobility and have characteristic appearances on DWI (i.e., an abscess has reduced diffusion and appears DWI hyperintense, and ADC hypointense). DWI with ADC maps provide additional information for better characterization of PNS infections aiding in evaluation of different complications, including abscess, by differentiating serous fluid, pus, and intravascular infectious thrombophlebitis ***(19).***

Acute Rhinosinusitis and its Complications:

Most cases of ARS develop after a viral upper respiratory tract infection (including COVID-19). The typical symptoms include fever and two or more of the following: discoloured nasal discharge, midface pressure or pain, nasal blockage/obstruction/congestion, hyposmia, and cough. The viral infection causes mucosal congestion, which leads to obstruction of normal flow of the mucus within the PNS ***(20).***

This may facilitate bacterial superinfection. The typical symptoms of ARS include two or more of the following: discoloured nasal discharge, midface pressure or pain, nasal blockage/obstruction/congestion, hyposmia, and coughing. Viral ARS typically resolves in 7-10 days ***(21).***

Neuroimaging is not indicated for the evaluation of ARS unless complications are suspected. Most children with viral ARS can be diagnosed clinically, without the need for imaging studies. The clinical diagnosis in children may, however, be challenging because the distinction of symptoms from other inflammatory diseases of the upper respiratory tract is difficult, or symptoms are either subtle or nonspecific ***(16).***

- Bacterial Acute Rhinosinusitis:

BARS should be suspected in at least three potential clinical presentations. (1) Severe symptoms at onset: persistent high fever (greater or equal to 39 °C), purulent nasal discharge, and appearing ill for at least 3 days. (2) Worsening symptoms: increasing symptoms such as severe headache or fever 5 days after onset, frequently after initial apparent recovery; or (3) Persistent symptoms without improvement for more than 10 days and less than 20 days ***(15).***

Complications of BARS are caused by local or hematogenous spread of the infection. Thus, emergent imaging studies are often necessary in the evaluation of the complications of BARS. Several authors recommend performing CT on patients only when the symptoms persist for at least 10 days and/or if there is evidence of intracranial or orbital complications ***(20).***

The presence of air-fluid levels or complete opacification of the sinuses on CT studies is strongly associated with BARS. In addition, bubbles of air mixed with fluid/soft tissue density in the sinuses on CT are suggestive of BARS. MRI of the PNS, orbit, or brain should always be performed if there is suspicion of complications associated with BARS ***(21).***

- Orbital Complications:

Orbital complications are commonly associated with BARS. The close proximity of the ethmoid complexes to the orbit allows for direct infectious spread through gaps in the thin lamina papyracea. The orbital complications are categorized by the Chandler staging which is based on CT findings, with preseptal cellulitis (stage I) commonly seen after BARS presenting with edema, erythema, and tenderness of the upper eyelid ***(17).***

Extraocular movements and visual acuity remain intact in stage I. Orbital cellulitis (stage II) can have a similar symptom profile but can rapidly progress to subperiosteal (stage III) or orbital abscess. Chemosis, exophthalmos, visual impairment, and ophthalmoplegia are typically secondary due to the mass effect of an abscess. Subperiosteal abscess are typically located medially along the lamina papyracea for ethmoid sinusitis and superiorly or superomedially for frontal or frontoethmoidal sinusitis (***15).***

Thrombophlebitis of the orbital veins (e.g., superior ophthalmic vein) may lead to cavernous sinus thrombosis (CST) (stage V) which may be considered both an orbital and intracranial complication. If not treated early and aggressively, CST can lead to severe retroorbital pain, high fever, meningitis, ophthalmoplegia, blindness, stroke, or even death ***(19).***

CT is excellent for determining whether there is intraorbital extension of PNS disease into the ventral two thirds of the orbit. However, when the infection approaches the orbital apex, an MRI study with contrast is necessary to assess spread into the cavernous sinus and the intracranial compartment. Intraorbital extension of PNS disease can be detected by imaging either as a diffuse infiltration of the orbital fat or as periorbital inflammation, subperiosteal abscess, or a true orbital abscess ***(16).***

- Intracranial Complications:

Intracranial complications of BARS are less common in the postantibiotic era, but they are still the most serious and morbid complications of patients. The majority of patients are young adolescent males (70%). Hematogenous/vascular spread (retrograde thrombophlebitis via the diploic veins) is the main route of the infection spread, but direct spread of the infection is also possible ***(17).***

Intracranial complications are classified as meningitis (most common), epidural abscess, subdural empyema, CST, and intracerebral abscesses. It is not rare for a patient with PNS disease and complications to present with more than one focus of infection; intracranial or orbital, or both. Patients most often present with nonspecific symptoms such as headache, fever, nausea, and vomiting. Therefore, neuroimaging is essential to assess these cases ***(20).***

MRI with contrast administration is superior to CT and confirms the diagnosis when intracranial complications are suspected. Intracranial complications rarely occur in isolation. The usual potential sources of infection are sphenoid and/or ethmoid BARS for meningitis, frontal BARS for epidural abscess formation, frontal BARS for subdural empyema, sphenoid and/or ethmoid and/or frontal BARS for CST and frontal and/or ethmoid BARS for intracerebral abscess ***(17).***

The recognition of various patterns of meningeal enhancement (leptomeningeal vs pachymeningeal) on postcontrast MRI is helpful in differentiating between infectious and carcinomatous meningitis, or intracranial hypotension. Meningitis presents mostly as regional or diffuse leptomeningeal contrast enhancement, while carcinomatous meningitis presents as focal leptomeningeal or pachymeningeal contrast enhancement ***(17).***

Epidural abscess and subdural empyema present as extra-axial fluid collections with an enhancing rim between the skull and the brain parenchyma with mass effect on the adjacent brain and reactive edema. If the infectious fluid collection crosses the fall, it is located epidural, if it is limited to one side of the falx, it is either subdural or epidural ***(15).***

Infection spread from the extra-axial space to the brain parenchyma can lead to focal cerebritis and subsequently intracerebral abscess formation which can be seen both on CT and MRI as a fluid collection with a well-defined enhancing rim with mass effect and prominent swelling of adjacent brain parenchyma. Concomitant thrombophlebitis may also contribute to the intracranial extension of the epidural or subdural empyema, possibly complicated by a venous stroke secondary to a phlebothrombosis ***(20).***

Typical treatment methods are surgical incision and drainage, combined with a long course of intravenous antibiotic treatment. Frontal sinus BARS, and anaerobic and polymicrobial sinus cultures are predictive of a more severe infection requiring more surgical interventions, prolonged intravenous antibiotic treatment, and overall hospital length of stay ***(19).***

Chronic Rhinosinusitis and its Complications:

CRS (with or without sinonasal polyposis) is also relatively common in children and due to the subtle and nonspecific symptoms, it is usually overlooked. The main factors causing CRS are the immune deficiencies. CT is the gold standard to guide diagnosis and management of CRS. CT findings of CRS typically include mucosal thickening, bony remodelling, polyposis, mucus retention cysts, and bone thickening secondary to osteitis from adjacent chronic mucosal inflammation ***(16).***

Figure (3): Coronal CT scan in bone-window algorithm of a patient with chronic rhinosinusitis. This image reveals moderate mucosal thickening in the right maxillary sinus and mild mucosal thickening in the left maxillary sinus ***(22).***

- Odontogenic Sinusitis:

Odontogenic sinusitis is an inflammatory condition of the PNS that is the result of dental pathology. Odontogenic sinusitis may be acute or chronic. The teeth should always be evaluated for etiologies of the inflammation including periapical abscess or osseous lesions including defects or roots extending into the maxillary sinuses ***(23).***

Fungal Rhinosinusitis:

Although rare, the frequency of fungal sinusitis in children has been increasing over the past decades. Interactions between fungi and the PNS result in a range of clinical presentations with a broad spectrum of clinical severity. Neuroimaging plays an important role in the diagnosis of FRS. FRS is most commonly classified into invasive and non-invasive subtypes based on histopathological evidence of tissue invasion ***(24).***

- Invasive Fungal Rhinosinusitis:

Invasive fungal rhinosinusitis (IFRS) is categorized into acute or chronic invasive and chronic granulomatous forms. Chronic IFRS preferentially affects the ethmoid and sphenoid sinuses and although rarely it occurs in immunocompetent children. Acute IFRS is a relatively rare, aggressive, sometimes life-threatening submucosal infiltration of fungal organisms in the nasal cavity and PNS. In the general population, the acute IFRS mortality rate is quite high and reaches up to 50-61% of the patients (***24).***

Acute IFRS most frequently develops in immunocompromised patients (i.e., due to hematologic malignancies, secondary to chemotherapy, chronic immunosuppressive drug therapies, poorly controlled diabetes mellitus, malnutrition, and corticosteroid treatment). The initial presentation is nonspecific, but typical symptoms are persistent fevers, congestion, and rhinorrhea in an immunocompromised patient ***(18).***

Typical findings on rhinoscopy or endoscopy are pale and greyish nasal mucosa and bloody crusts. Painless nasal septal necrosis is frequent on presentation. The IFRS may spread into the orbits, meninges, and brain from the nasal cavity and PNS by direct extension. CT scan can show the extent of PNS involvement, however, MRI is superior in the diagnosis of intraorbital and intracranial involvement ***(25).***

Unilateral nasal cavity mucosal thickening is the earliest CT finding of IFRS; severe thickening of the nasal mucosa along the turbinates, nasal walls and septum is seen in most cases.48 A recent study on MRI of acute IFRS showed that extrarhinosinusal involvement is common and the orbit (65.2%) is the most commonly involved location ***(16).***

In addition, a relative lack of contrast enhancement was correlated with coagulation necrosis and was a unique prognostic factor that linked to worse survival in those cases. Finally, the lack of contrast enhancement in the nasal cavity due to mucosal necrosis occurs in patients with mucormycosis, due to its angioinvasive nature ***(26).***

- Noninvasive Fungal Rhinosinusitis:

Noninvasive FRS is categorized as allergic FRS, fungal ball, and localized asymptomatic fungal colonization. Allergic FRS is the most common form of FRS. It usually affects young immunocompetent

patients who present with chronic PNS infection proptosis and polyposis and a history of previous sinus surgery **(26).**

The diagnosis of allergic FRS depends on characteristic imaging findings: bilateral, multisinus involvement is the most common presentation, however, unilateral multi- or pansinus involvement may also be seen. The classical CT findings in allergic FRS is the "double density" sign which is due to thick fungal mucin (which may contain heavy metal deposits) surrounded by mucosal thickening and peripheral enhancement **(18).**

Also, the high protein concentration of allergic mucin causes central T1-low signal and T2-signal void. Fungal balls were previously termed as mycetomas or aspergillomas, owing to the most commonly encountered fungus being. Other fungi have been associated with fungal ball production justifying the change in terminology. The presentation of a fungal ball is usually nonspecific and asymptomatic **(25).**

Fungal balls are diagnosed histologically. On CT scans, fungal balls are suspected within an opacified sinus with intralesional hyperdensity or calcification. MRI features of fungal balls are central T1/T2-hypointensity (calcification) surrounded by T2-hyperintensity (hypertrophic mucosal walls of the PNS) sometimes indistinguishable from nonfungal chronic sinusitis with central normal sinus air **(18).**

Imaging of Rhino-orbito-cerebral Mucormycosis

CT and MRI help in making an early pre-operative diagnosis of ROCM. Imaging plays a vital role in evaluation of disease spread which in turn guides medical and surgical management. CT is quick and readily available; common findings include opacification of the sinonasal air spaces and obliteration of the deep neck fat pads. Bone destruction, if any, is best identified on CT bone algorithms. MRI, with its excellent inherent soft tissue resolution, helps in characterising sinonasal contents, involvement of the deep neck soft tissues and spaces as well as identify perineural and intracranial spread. In an appropriate clinical setting, the imaging features of ROCM are diagnostic [22].

For the ease of reporting, we classify ROCM into 2 broad categories, based on anatomic involvement: sinonasal (nasal cavity and paranasal sinuses) and extra-sinus (deep neck, orbital and intracranial) involvement. A detailed account of the previously reported literature and pertinent imaging features of ROCM is presented.

Sinonasal involvement

ROCM typically begins in the nasal mucosa and spreads into the paranasal sinuses [23]. CT findings of nasal MCR are non-specific and sparsely reported. In a study to characterise CT findings in invasive fungal sinusitis (IFS) (mucormycosis, aspergillosis), DelGaudio et al. found severe thickening of the nasal mucosa, turbinates, septum and nasal floor in 91% (21/23) patients [24]. CT may also reveal isolated, non-specific turbinate hypertrophy with/without inflammatory fluid [2]. Nasal septal perforation has been identified by Therakathu et al. in ROCM [2].

At MRI, the involved nasal mucosa may demonstrate varied signals, including hyperintensity (necrosis) or hypointensity (fungal paramagnetic material) on T2W images [2, 25]. Safder et al. reported 2 cases with restricted diffusion, in the turbinates and mucoperiosteal thickening within the maxillary sinus, representing infarcted tissue [25]. Necrosis and devitalisation of the turbinates may cause lack of contrast enhancement on MRI. This appearance is termed as the "black turbinate (BT) sign" [25] (Fig. 5). The BT sign was first described in nasal MCR, but subsequently reported in other cases of IFS [25, 26].

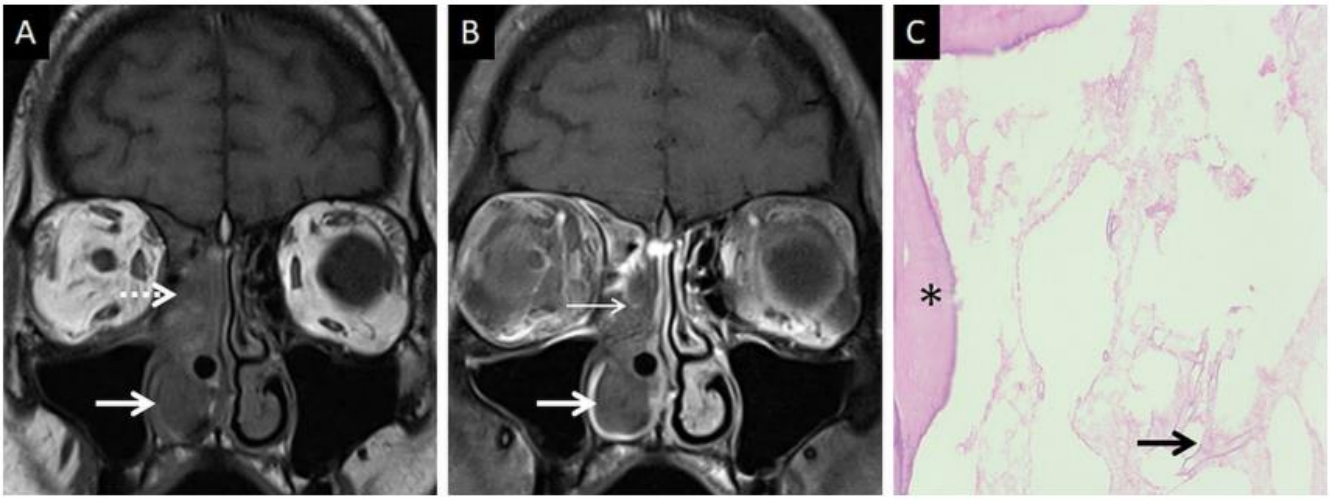

Figure 4: Classic appearance of the "black turbinate" sign. Unenhanced coronal T1W image (a) reveals intermediate signal contents within the rightnasal cavity (dotted arrow) and hypertrophy of the right inferior turbinate (thick arrow). Corresponding CE fat-suppressed (FS) coronal T1W image (b) reveals poor enhancement of the right middle (thin arrow) and inferior turbinates (thick arrow) due to necrosis, resulting in the "black turbinate" sign. Post-operative histopathology analysis (c), using HE staining, demonstrates necrosis of the turbinate (*) and branching, aseptate fungal hyphae (thick arrow) consistent with the diagnosis of MCR

It is worthwhile to note that this imaging appearance has been identified in normal subjects as well [33]. The lack of enhancement in normal subjects is linked to the normal cavernous tissues within the turbinates [27]. Involvement of the posterior portions of the inferior and middle turbinates, well-defined margins, hyperintense T2 signals, thin peripheral enhancement, progressive enhancement on dynamic contrast-enhanced scans and T2 hyperintensity favour benign BT [27]. On the contrary, fungal BTs are confluent, ill defined, non-enhancing masses commonly involving the middle turbinate (because they filter majority of nasal airflow) [27, 28].

Involvement of the paranasal sinuses is common. In studies on ROCM, Bhansali et al., Ferry et al. and Yohai et al. reported PNS involvement in 100%, 69% and 79% patients, respectively [23, 29, 30]. Some authors identify the maxillary sinus to be most frequently involved; others suggest the ethmoid sinuses [2, 22]. Involvement of multiple sinuses is common; maxillary, ethmoid and sphenoid sinuses being a common combination [2]. In a study on 43 patients with proven ROCM by Therakathu et al., unilateral sinus involvement was found to be more common; however, in another study by Slonimsky et al. bilateral sinonasal involvement was found more in ROCM than aspergillosis [2, 31].

CT features of paranasal sinus disease in ROCM include a rind of soft tissue, dense opacification or variable, nodular, mucoperiosteal thickening [28, 31]. The presence of air fluid levels have been disputed in the literature [22, 25, 32]. Radiodense concretions, common in aspergillosis, are not seen in ROCM [33]. MRI signals of the sinus contents may vary, ranging from hyperintensity to profound hypointensity (due to fungal paramagnetic contents) on T2W images [22, 32] Contrast-enhanced scans also reveal range of enhancement patterns, including absent to heterogeneous intense enhancement [2] Bacterial sinusitis lacks local necrosis, hence, the mucosal T2 signals and enhancement are not affected [34].

Extra-sinus spread

Extra-sinus extension of the MCR is common, often without radiological evidence of bony sinus wall destruction [32]. Bone destruction in the ROCM has been found in only 40% cases [16]. The angioinvasive propensity of the fungus, and its ability to disseminate along the perivascular channels, allows the invasion of adjacent structures through intact bony partitions [35] If involved, the bones may show rarefaction, erosions or permeative destruction on a CT scan [2].

Deep neck involvement

Stranding and/or soft tissue obliteration of the fat planes are important signs of fungal spread into the deep neck spaces [36]. Involvement of the distinct fat planes anterior and posterior to the maxillary sinus (anterior periantral fat and posterior periantral/retro-antral fat, respectively) is common. Retro-antral fat involvement is considered to be one of the initial imaging signs of deep neck invasion in ROCM [37, 38] Stranding or soft tissue in the periantral region is thought to be due to congestive oedema secondary to vascular thrombosis or the presence of fungal elements due to spread along blood vessels and perivascular spaces across the confines of the maxillary sinus [37]. Irrespective of the nature of the soft tissue, this region is an important review area, especially if dedicated CT/MRI of the neck is not performed

The pterygopalatine fossa (PPF) may also be involved, due to spread from the nasal cavity via the sphenopalatine foramen [39]. Middlebrooks et al. suggested that involvement of the PPF correlated strongly with acute IFS ($r = 0.64$) and sphenopalatine foramen involvement was present in 72% of patients [40].

Normally, fat is seen around the branches of the internal maxillary artery in the PPF [36]. Obliteration of this fat must raise suspicion for extension of the infection [36] (Fig. 9). In our literature search, involvement of the deep neck spaces, including the PPF, have only occasionally been alluded to. In a case series of 10 patients with ROCM, involvement of the PPF was seen in all patients. Accounting for this, the authors suggested routine exploration of the PPF during surgical debridement in patients with ROCM [39]. Owing to the aggressive spread of MCR and the extensive communication of the PPF with other vital structures (oral cavity, orbit, middle cranial fossa), we recommend inclusion of dedicated neck imaging studies in all patients with suspected ROCM coupled with a thorough evaluation of the PPF in each case.

In furtherance of the review of the deep neck spaces, we also suggest evaluation of the skull base. Skull base osteomyelitis (SBO) is rare in ROCM, even in the presence of deep neck involvement [22]. SBO in ROCM has been recorded in the chronic phase of the infection [2, 22]. However, we encountered one patient presenting with acute cranial nerve palsies with radiological evidence as well as pathologically proven SBO Marrow signal alterations, seen as hypointense on T1W and hyperintense on STIR images, are features typical of SBO [22, 41]. MCR-related SBO may reveal abnormal heterogeneous marrow enhancement with non-enhancing areas representing devitalised bone on contrast-enhanced (CE) MRI [41].

Orbital involvement

Orbital involvement results from spread of MCR via the nasolacrimal duct and lamina papyracea [23]. Spread may also occur from the PPF via the inferior orbital fissure [39]. Independent studies on ROCM, yielded an incidence of orbital invasion ranging between 76 and 80% [2, 23].

Orbital soft tissue, similar to PNS contents, is a typical imaging feature of intraorbital MCR spread [2]. Orbital fat stranding, including the retro-bulbar region, as well as thickening and/or displacement of the medial rectus (indicating spread from ethmoid sinuses) are also frequently encountered [22, 48] (Fig. 13). Proptosis may occur due to retro-bulbar inflammation and/or orbital apex involvement [22, 39]. Orbital apex involvement occurs due to spread from the sphenoid sinuses and forms an important conduit for intracranial spread [49]. MCR is the most common aetiology of orbital apex syndrome among all fungal infections [49].

Occlusion of the orbital vessels (superior ophthalmic vein, ophthalmic artery), due to MCR-related vasculitis and thrombosis, may also be noted [22]. The occlusion of the ophthalmic artery and/or central retinal artery may result in optic nerve infarction (ONI). In our literature review, we found 7 previously published reports of ONI in patients with ROCM [50–56]. Of these, there were 2 reports of bilateral ONI and 1 report of ONI being the initial presentation of orbital MCR [51, 52, 55]. Infarcted optic nerves demonstrates restricted diffusion and normal FLAIR signals on MRI [51] (Fig. 5).

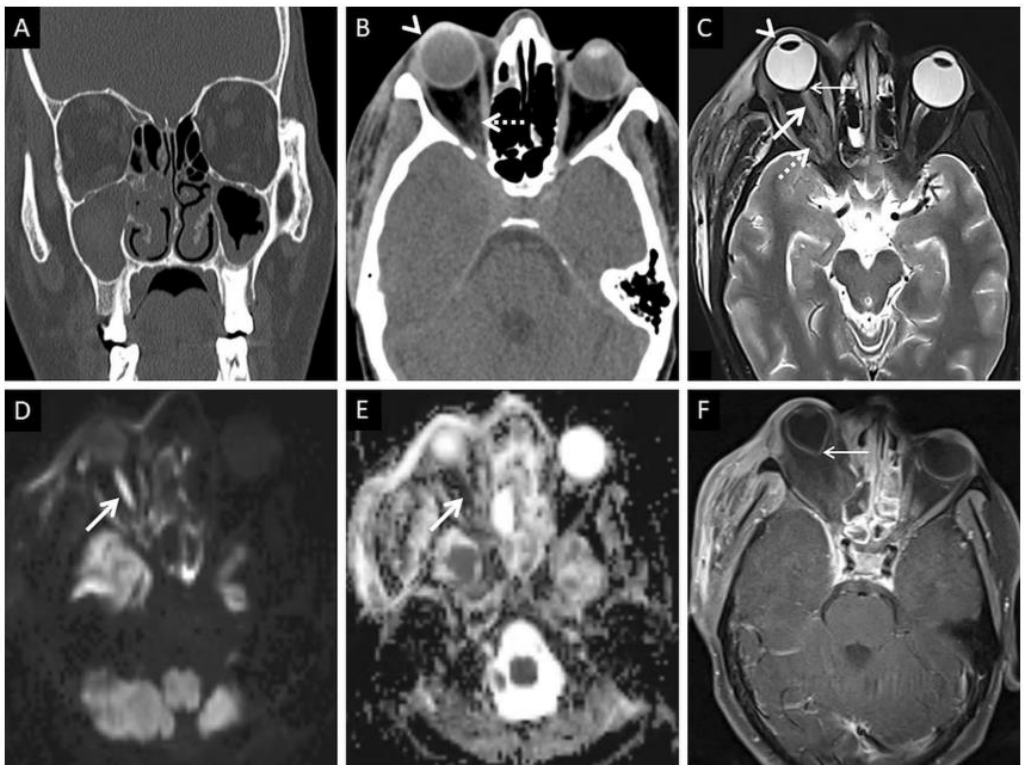

Figure 5: ROCM-related ONI and endophthalmitis. Coronal CT image of the paranasal sinuses (a), obtained using the bone algorithm, reveals opacifcation of the maxillary sinuses, worse on the right. Axial CT image (b), using the soft tissue algorithm, demonstrates subtle right orbital fat stranding (dotted arrow) and mild right proptosis (arrow head). Axial T2-FS image (c) confrms the right orbital stranding (dotted arrow) and right proptosis (arrow head). Note the subtle tenting of the posterior aspect of the right globe (thin arrow) and thickening of the right optic nerve (thick
arrow). Axial difusion weighted (d) and apparent difusion coefcient (e) images reveal restricted difusion within the right optic nerve in keeping with an optic nerve infarction. Overall, fndings of orbital compartment syndrome with endophthalmitis and optic nerve infarction was suggested. The patient underwent urgent surgery, with removal of the right lamina papyracae, for relief of the compartment syndrome. CE FS axial T1W image(f) reveals interim worsening of the right endophthalmitis (thin arrow)

Conflicts of Interest: The authors declare no conflict of interest.

References

1. Shankar, L., & Evans, K. (2021). An atlas of imaging of the paranasal sinuses. CRC Press.
2. Iida, E., & Anzai, Y. (2017). Imaging of paranasal sinuses and anterior skull base and relevant anatomic variations. Radiologic Clinics, 55(1), 31-52.
3. Kanwar, S. S., Mital, M., Gupta, P. K., Saran, S., Parashar, N., & Singh, A. (2017). Evaluation of paranasal sinus diseases by computed tomography and its histopathological correlation. Journal of Oral and Maxillofacial Radiology, 5(2), 46.
4. Wuest, W., May, M., Saake, M., Brand, M., Uder, M., & Lell, M. (2016). Low-dose CT of the paranasal sinuses: minimizing X-ray exposure with spectral shaping. European radiology, 26, 4155-4161.
5. Shpilberg, K. A., Daniel, S. C., Doshi, A. H., Lawson, W., & Som, P. M. (2015). CT of anatomic variants of the paranasal sinuses and nasal cavity: poor correlation with radiologically significant rhinosinusitis but importance in surgical planning. American Journal of Roentgenology, 204(6), 1255-1260.
6. Fatterpekar, G., Chen, S., Pramanik, B., Hagiwara, M., Galheigo, D. (2013). Radiologic Evaluation/Diagnostic Imaging of Paranasal Sinuses and Chronic Rhinosinusitis. In: Kountakis, S.E. (eds) Encyclopedia of Otolaryngology, Head and Neck Surgery. Springer, Berlin, Heidelberg.
7. Wucherpfennig, L., Triphan, S. M., Wege, S., Kauczor, H. U., Heussel, C. P., Schmitt, N., ... & Wielpütz, M. O. (2022). Magnetic resonance imaging detects improvements of pulmonary and paranasal sinus abnormalities in response to

elexacaftor/tezacaftor/ivacaftor therapy in adults with cystic fibrosis. Journal of Cystic Fibrosis, 21(6), 1053-1060.

8. Munhoz, L., Júnior, R. A., Abdala, R., & Arita, E. S. (2018). Diffusion-weighted magnetic resonance imaging of the paranasal sinuses: a systematic review. Oral surgery, oral medicine, oral pathology and oral radiology, 126(6), 521-536.
9. Gupta, V., Prabhakar, A., Yadav, M., & Khandelwal, N. (2019). Computed tomography imaging-based normative orbital measurement in Indian population. Indian journal of ophthalmology, 67(5), 659.
10. Liza, C. M., & Yoon, M. K. (2019). Update on current aspects of orbital imaging: CT, MRI, and ultrasonography. International ophthalmology clinics, 59(4), 69-79.
11. Shah, S. M., Kilgore, K. P., Bothun, E. D., Hunt, C. H., & Khanna, C. L. (2022). Orbital anatomy magnetic resonance imaging in diplopic versus non-diplopic patients after glaucoma drainage device placement. European Journal of Ophthalmology, 32(1), 341-346.
12. Rana, K., Juniat, V., Rayan, A., Patel, S., & Selva, D. (2022). Normative measurements of orbital structures by magnetic resonance imaging. International Ophthalmology, 42(12), 3869-3875.
13. Cameron, J. R., & Tatham, A. J. (2016). A window to beyond the orbit: the value of optical coherence tomography in non-ocular disease. Acta Ophthalmologica, 94(6), 533-539.
14. Khazaei, H., Khazaei, D., Ashraf, D., Mikkilineni, S., & Ng, J. D. (2022). Overview of Orbital Ultrasonography. survival, 9, 10.
15. Casanueva, R., Villanueva, E., Llorente, J. L., & Coca-Pelaz, A. (2022). Management options for orbital complications of acute rhinosinusitis. American Journal of Otolaryngology, 43(3), 103452.
16. Orman, G., Kralik, S. F., Desai, N., Meoded, A., Vallejo, J. G., Huisman, T. A., & Tran, B. H. (2020). Imaging of paranasal sinus infections in children: a review. Journal of Neuroimaging, 30(5), 572-586.
17. Bhatt, A. A., Donaldson, A. M., Olomu, O. U., Gupta, V., & Sandhu, S. J. S. (2020). Can Diffusion-Weighted Imaging Serve as an Imaging Biomarker for Acute Bacterial Rhinosinusitis?. Cureus, 12(8).
18. Mossa, M., Ilica, A. T., Maluf, F., Karakoç, Ö., İzbudak, İ., & Aygün, N. (2013). The many faces of fungal disease of the paranasal sinuses: CT and MRI findings. Diagnostic and Interventional Radiology, 19(3), 195.
19. Lloyd, G. A. (2012). Diagnostic imaging of the nose and paranasal sinuses. Springer Science & Business Media.
20. Ebell, M. H., McKay, B., Dale, A., Guilbault, R., & Ermias, Y. (2019). Accuracy of signs and symptoms for the diagnosis of acute rhinosinusitis and acute bacterial rhinosinusitis. The Annals of Family Medicine, 17(2), 164-172.
21. Autio, T. J., Koskenkorva, T., Närkiö, M., Leino, T. K., Koivunen, P., & Alho, O. P. (2016). Imaging follow-up study of acute rhinosinusitis. The Laryngoscope, 126(9), 1965-1970.
22. Chamilos G, Lewis RE, Kontoyiannis DP. Delaying amphotericin B-based frontline therapy significantly increases mortality among patients with hematologic malignancy who have zygomycosis. *Clin Infect Dis.* 2008;47:503–509. [PubMed] [Google Scholar]
23. Chan LL, Singh S, Jones D, Diaz EM, Jr, Ginsberg L. Imaging of mucormycosis skull base osteomyelitis. *AJNR Am J Neuroradiol.* 2000;21(5):828–831. [PMC free article] [PubMed] [Google Scholar]
24. Bhansali A, Bhadada S, Sharma A, et al. Presentation and outcome of rhino-orbital-cerebral mucormycosis in patients with diabetes. *Postgrad Med J.* 2004;80(949):670–674. [PMC free article] [PubMed] [Google Scholar]
25. DelGaudio JM, Swain RE, Jr, Kingdom TT, Muller S, Hudgins PA. Computed tomographic findings in patients with invasive fungal sinusitis. *Arch Otolaryngol Head Neck Surg.* 2003;129(2):236. [PubMed] [Google Scholar]
26. Safder S, Carpenter JS, Roberts TD, Bailey N. The "Black Turbinate" sign: an early MR imaging finding of nasal mucormycosis. *AJNR Am J Neuroradiol.* 2009;31(4):771–774. [PMC free article] [PubMed] [Google Scholar]
27. Horger M, Hebart H, Schimmel H, et al. Disseminated mucormycosis in haematological patients: CT and MRI findings with pathological correlation. *Br J Radiol.* 2006;79(945):88–e95. [PubMed] [Google Scholar]
28. Han Q, Escott E. The black turbinate sign, a potential diagnostic pitfall: evaluation of the normal enhancement patterns of the nasal turbinates. *AJNR Am J Neuroradiol.* 2019;40(5):855–861. [PMC free article] [PubMed] [Google Scholar]
29. Gillespie MB, O'Malley BW, Jr, Francis HW. An approach to fulminant invasive fungal rhinosinusitis in the immunocompromised host. *Arch Otolaryngol Head Neck Surg.* 1998;124:520–526. [PubMed] [Google Scholar]
30. Ferry AP, Abedi S. Diagnosis and management of rhino-orbitocerebral mucormycosis (phycomycosis): a report of 16 personally observed cases. *Ophthalmology.* 1983;90(9):1096–1104. [PubMed] [Google Scholar]
31. Yohai RA, Bullock JD, Aziz AA, Markert RJ. Survival factors in rhino-orbital-cerebral mucormycosis. *Surv Ophthalmol.* 1994;39(1):3–22. [PubMed] [Google Scholar]
32. Slonimsky G, McGinn JD, Goyal N, et al. A model for classification of invasive fungal rhinosinusitis by computed tomography. *Sci Rep.* 2020;10(1):12591. [PMC free article] [PubMed] [Google Scholar]
33. Rumboldt Z, Castillo M. Indolent intracranial mucormycosis: case report. *AJNR Am J Neuroradiol.* 2002;23(6):932–934. [PMC free article] [PubMed] [Google Scholar]
34. Peterson KL, Wong M, Canalis RF, Abemayor E. Rhinocerebral mucormycosis: evolution of the disease and treatment options. *Laryngoscope.* 1997;107:855–862. [PubMed] [Google Scholar]
35. Nunes DM, Rocha AJ, Rosa Júnior MR, da Silva CJ. "Black turbinate sign": a potential predictor of mucormycosis in

cavernous sinus thrombophlebitis. *Arq Neuropsiquiatr.* 2012;70(1):78. [PubMed] [Google Scholar]

36. Aribandi M, McCoy VA, Bazan C. Imaging features of invasive and noninvasive fungal sinusitis: a review. *Radiographics.* 2007;27(5):1283–1296. [PubMed] [Google Scholar]
37. Gamba JL, Woodruff WW, Djang WT, Yeates AE. Craniofacial mucormycosis: assessment with CT. *Radiology.* 1986;160(1):207–212. [PubMed] [Google Scholar]
38. Silverman CS, Mancuso AA. Periantral soft-tissue infiltration and its relevance to the early detection of invasive fungal sinusitis: CT and MR findings. *AJNR Am J Neuroradiol.* 1998;19:321–325. [PMC free article] [PubMed] [Google Scholar]
39. Mossa-Basha M, Turan Ilıca A, Maluf F, Karakoç O, İzbudak I, Aygün N. The many faces of fungal disease of the paranasal sinuses: CT and MRI findings. *Diagn Interv Radiol.* 2013;19:195–200. [PubMed] [Google Scholar]
40. Hosseini SMS, Borghei P. Rhinocerebral mucormycosis: pathways of spread. *Eur Arch Otorhinolaryngol.* 2005;262(11):932–938. [PubMed] [Google Scholar]
41. Middlebrooks EH, Frost CJ, De Jesus RO, Massini TC, Schmalfuss IM, Mancuso AA. Acute invasive fungal rhinosinusitis: a comprehensive update of CT findings and design of an effective diagnostic imaging model. *AJNR Am J Neuroradiol.* 2015;36(8):1529–1535. [PMC free article] [PubMed] [Google Scholar]
42. Chapman PR, Choudhary G, Singhal A. Skull base osteomyelitis: a comprehensive imaging review. *AJNR Am J Neuroradiol.* 2021;42(3):404–413. [PMC free article] [PubMed] [Google Scholar]
43. McLean FM, Ginsberg LE, Stanton CA. Perineural spread of rhinocerebral mucormycosis. *AJNR Am J Neuroradiol.* 1996;17:114–116. [PMC free article] [PubMed] [Google Scholar]
44. Frater JL, Hall GS, Procop GW. Histologic features of zygomycosis. Emphasis on perineural invasion and fungal morphology. *Arch Pathol Lab Med.* 2001;125:375–378. [PubMed] [Google Scholar]
45. Sravani T, Uppin SG, Uppin MS, Sundaram C. Rhinocerebral mucormycosis: pathology revisited with emphasis on perineural spread. *Neurol India.* 2014;62(4):383–386. [PubMed] [Google Scholar]
46. Press GA, Weindling SM, Hesselink JR, Ochi JW, Harris JP. Rhinocerebral mucormycosis: MR manifestations. *J Comput Assist Tomogr.* 1988;12:744–749. [PubMed] [Google Scholar]
47. Orguc S, Yücetürk AV, Akif Demir M, Goktan C. Rhinocerebral mucormycosis: Perineural spread via the trigeminal nerve. *J Clin Neurosci.* 2005;12(4):484–486. [PubMed] [Google Scholar]
48. Dankbaar JW, Pameijer FA, Hendrikse J, Schmalfuss IM. Easily detected signs of perineural tumour spread in head and neck cancer. *Insights Imaging.* 2018;9:1089–1095. [PMC free article] [PubMed] [Google Scholar]
49. Bae MS, Kim EJ, Lee KM, Choi WS. Rapidly progressive rhino-orbito-cerebral mucormycosis complicated with unilateral internal carotid artery occlusion: a case report. *Neurointervention.* 2012;7(1):45–49. [PMC free article] [PubMed] [Google Scholar]
50. Anders UM, Taylor EJ, Martel JR, Martel JB. Acute orbital apex syndrome and rhino-orbito-cerebral mucormycosis. *Int Med Case Rep J.* 2015;8:93–96. [PMC free article] [PubMed] [Google Scholar]
51. Chaulk AL, Do TH, Supsupin EP, Bhattacharjee MB, Richani K, Adesina OOO. A unique radiologic case of optic nerve infarction in a patient with mucormycosis. *J Neuroophthalmol.* 2021 doi: 10.1097/WNO.0000000000001179. [PubMed] [CrossRef] [Google Scholar]
52. Ghuman MS, Kaur S, Bhandal SK, Ahluwalia A, Saggar K. Bilateral optic nerve infarction in rhino-cerebral mucormycosis: A rare magnetic resonance imaging finding. *J Neurosci Rural Pract.* 2015;6(3):403–404. [PMC free article] [PubMed] [Google Scholar]
53. Alsuhaibani AH, Al-Thubaiti G, Al Badr FB. Optic nerve thickening and infarction as the first evidence of orbital involvement with mucormycosis. *Middle East Afr J Ophthalmol.* 2012;19(3):340–342. [PMC free article] [PubMed] [Google Scholar]
54. Mathur S, Karimi A, Mafee MF. Acute optic nerve infarction demonstrated by diffusion-weighted imaging in a case of rhinocerebral mucormycosis. *AJNR Am J Neuroradiol.* 2007;28(3):489–490. [PMC free article] [PubMed] [Google Scholar]
55. Lee BL, Holland GN, Glasgow BJ. Chiasmal infarction and sudden blindness caused by mucormycosis in AIDS and diabetes mellitus. *Am J Ophthalmol.* 1996;122(6):895–896. [PubMed] [Google Scholar]
56. Merkler AE, Duggal I, Kaunzner U, et al. Rapidly progressive bilateral optic nerve and retinal infarctions due to rhinocerebral mucormycosis and pseudoephedrine use. *Neurol Clin Pract.* 2016;6(6):549–552. [PMC free article] [PubMed] [Google Scholar]